INSTITUTE OF PHYSICS PUBLISHING CLASSICAL AND QUANTUM GRAVITY

Class. Quantum Grav. **22** (2005) S199–S208 doi:10.1088/0264-9381/22/10/010

# Technology developments for ACIGA high power test facility for advanced interferometry

**P Barriga[1], M Barton[2], D G Blair[1], A Brooks[3], R Burman[1], R Burston[4], E J Chin[1], J Chow[5], D Coward[1], B Cusack[5], G de Vine[5], J Degallaix[1], J C Dumas[1], M Feat[1], S Gras[1], M Gray[5], M Hamilton[3], D Hosken[3], E Howell[1], J S Jacob[1], L Ju[1], T L Kelly[3], B H Lee[1], C Y Lee[6], K T Lee[1], A Lun[4], D E McClelland[5], K McKenzie[5], C Mow-Lowry[5], A Moylan[5], D Mudge[3], J Munch[3], D Rabeling[5], D Reitze[7], A Romann[5], S Schediwy[1], S M Scott[5], A Searle[5], B S Sheard[5], B J J Slagmolen[1], P Veitch[3], J Winterflood[1], A Woolley[1], Z Yan[1] and C Zhao[6]**

[1] School of Physics, University of Western Australia, Perth, WA 6009, Australia
[2] California Institute of Technology, LIGO Project, Pasadena, CA 91125, USA
[3] Department of Physics, University of Adelaide, Adelaide, SA 5005, Australia
[4] Department of Mathematical Science, Monash University, Melbourne, VIC 3800, Australia
[5] Department of Physics, Faculty of Science, Australian National University, Canberra, ACT 0200, Australia
[6] Computer and Information Science, Edith Cowan University, Perth, WA 6050, Australia
[7] Department of Physics, University of Florida, Gainesville, FL 32611, USA

E-mail: pbarriga@cyllene.uwa.edu.au

Received 22 October 2004, in final form 14 January 2005
Published 21 April 2005
Online at stacks.iop.org/CQG/22/S199

**Abstract**

The High Optical Power Test Facility for Advanced Interferometry has been built by the Australian Consortium for Interferometric Gravitational Astronomy north of Perth in Western Australia. An 80 m suspended cavity has been prepared in collaboration with LIGO, where a set of experiments to test suspension control and thermal compensation will soon take place. Future experiments will investigate radiation pressure instabilities and optical spring effects in a high power optical cavity with ∼200 kW circulating power. The facility combines research and development undertaken by all consortium members, whose latest results are presented.

PACS number: 04.80.Nn

(Some figures in this article are in colour only in the electronic version)

## 1. Introduction

In collaboration with the world gravitational wave community, the objectives of the Australian Consortium for Interferometric Gravitational Astronomy (ACIGA) are to undertake research and development aimed at improving the performance of present laser interferometer gravitational wave (GW) detectors through advanced designs to ultimate limits set by mechanics, quantum mechanics, lasers and optics.

As part of the research, ACIGA has built the High Optical Power Test Facility (HOPTF) on the site of the future Australian International Gravitational Observatory (AIGO) in Gingin, 90 km north of Perth in Western Australia. Three tests were designed in collaboration with the Laser Interferometer Gravitational-Wave Observatory (LIGO). The objective is to determine and measure the effects of high laser power in the test masses including thermal lensing due to losses in both the substrate and the coating, and optical spring effects due to radiation pressure.

These experiments are designed to provide experience in the operation of advanced laser interferometers which will require the conditions created in the Gingin test facility. The technology development necessary to achieve our goals includes new approaches to vibration isolation and facilities for high power laser operation. Radiation pressure, parametric instability, test mass developments and thermal lens compensation have also been assessed.

## 2. Lasers

High power lasers ($\sim$100 W) are under development for the next generation of advanced interferometric GW detectors [1, 2]. An important step in this development is the 10 W laser developed by Adelaide University that has been recently installed at the HOPTF in Gingin. The design strategy for high power lasers is based on a power scalable, diode laser pumped continuous-wave Nd:YAG laser using a stable–unstable resonator. The use of an unstable resonator allows the mode volume in the gain medium to be increased, which reduces wavefront distortion and losses due to birefringence. They also offer efficient energy extraction, good mode discrimination and good beam quality at high powers. It has also being shown that the quality of the laser beam produced by an unstable resonator is less sensitive to changes in the refractive power of a thermal lens than a stable resonator [3].

Previously, we have demonstrated 80 W output and that a stable/unstable resonator laser can be injection locked. However, the output power was limited by the non-uniform pumping of the gain medium [4]. In the current design, shown in figure 1, the gain medium is a composite slab, composed of diffusion-bonded layers of Nd-doped and undoped YAG, and the side faces are coated with a layer of $SiO_2$. The pump light is gradually absorbed as it propagates along the longitudinal axis of the slab, and the heat is removed from the slab by conduction cooling through the side faces. There is therefore minimal thermal lens in the unstable direction, allowing collimation of the unstable mode and thus good overlap of the mode with the pumped volume. The effect of the thermal lens in the stable direction is reduced by the zigzag of the mode [5].

## 3. Vibration isolation

Reduction of seismic vibration applies to the main Fabry–Perot cavities test masses, and to other mirrors like the input optics and the beam splitter. By reducing the vibrations even at frequencies below the GW detection band (10 Hz–1 kHz), we facilitate the locking of high finesse cavities. As a consequence we will need less force on the actuators to control them,

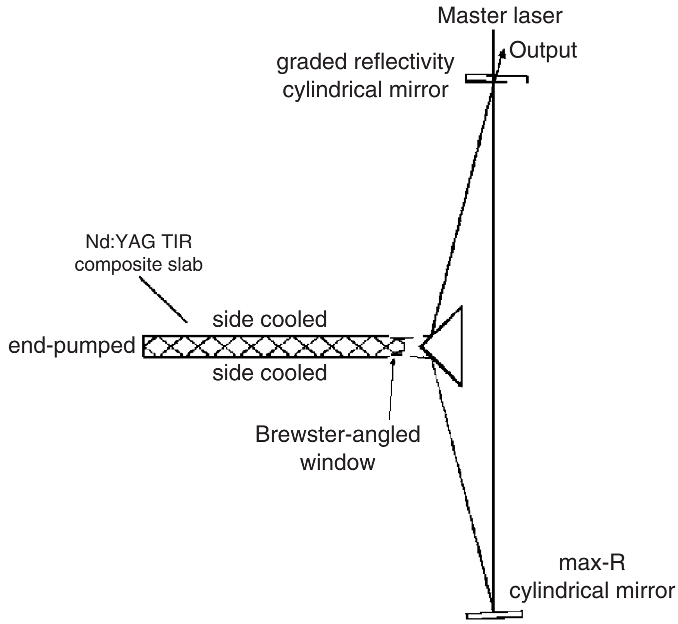


**Figure 1.** Schematic of the high power slave laser. The resonator is unstable in the direction perpendicular to the page and stable in the orthogonal direction.

reducing the servo forces needed to maintain the locking and also reducing the noise injection by them.

Actual GW detectors present diverse solutions in order to reduce seismic noise. Different materials and different combinations of isolation techniques including inverse pendulums [6, 7], cantilever blades [8] and multiple stage pendulums [9] are used to form complex isolation systems. In order to achieve the isolation requirements at low frequencies, different components and techniques have been developed by the University of Western Australia (UWA). A compact isolator structure includes two stages of horizontal pre-isolation, and one stage of vertical pre-isolation, all with resonant frequencies $\sim$30 mHz, so as to achieve residual motion at the nanometre levels. The isolator illustrated in figure 2(*a*) consists of an inverted pendulum horizontal stage cascaded with a LaCoste vertical stage [10]. The tilt rigidity of this structure allows us to cascade a Roberts Linkage [11] horizontal stage of pre-isolation, before the mounting of a four stage multi-pendulum system, where Euler springs for vertical suspension are included [12]. Each of the three intermediate masses is pivoted for self-damping as shown in the schematic of figure 2(*b*). The self-damping is achieved by mounting the pendulum masses from gimbals which allowed them to freely rock with respect to a short rigid section of the main pendulum chain, and then viscously coupling these two together with magnetic eddy current coupling.

## 4. Test masses

Present GW interferometers use fused silica as test mass substrate, but due to the high laser power needed for advanced GW detectors thermal effects play an important role. With higher thermal expansion coefficient and higher thermal conductivity $k$ (an advantage for future cryogenic detectors [13]), sapphire presents lower thermal gradient effects, which makes it

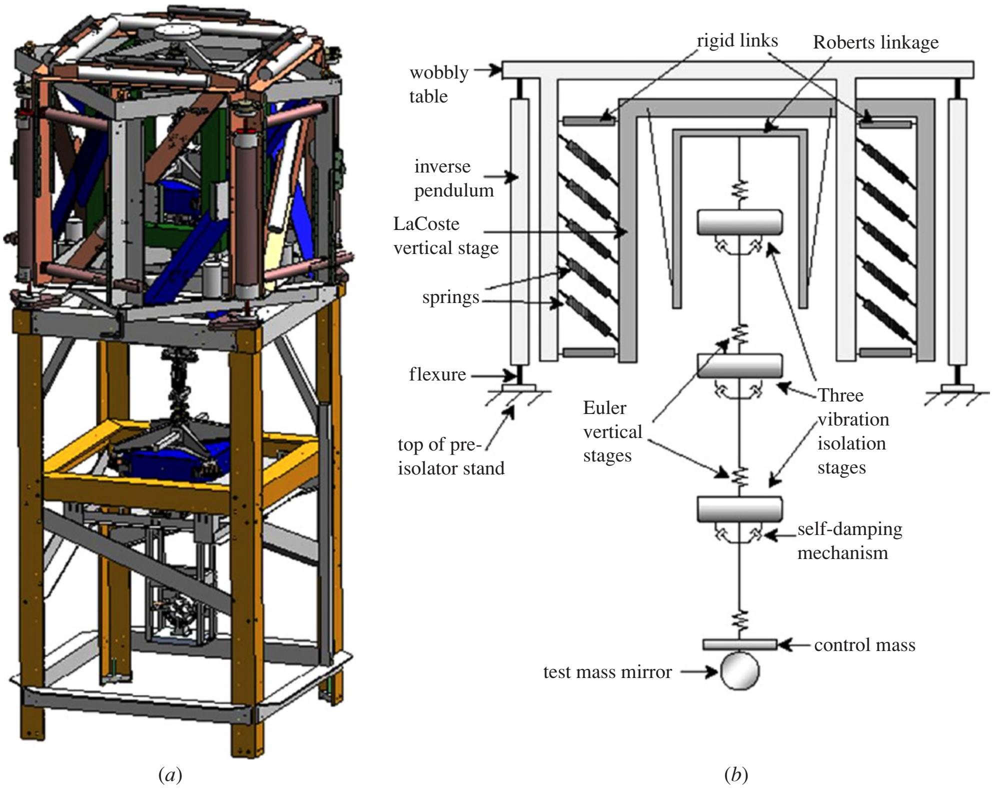


**Figure 2.** (*a*) Complete AIGO vibration isolation system with LIGO I suspension and test mass dummy as last stage. (*b*) Schematic diagram of the AIGO vibration isolation stack showing the three main sections: pre-isolation stage, multi-stage vibration isolation chain and the test mass.

more suitable for advanced GW detectors. Sapphire presents some problems as a test mass substrate due to scattering and relatively high optical absorption (higher than fused silica). Rayleigh scattering measurements have been conducted at UWA in order to characterize and improve the material with results showing inhomogeneous structures and point defects [14].

Sapphire's higher Q-factor indicates lower thermal noise. By changing the test mass substrate, it is difficult to use fused silica fibres as suspension material due to the differential thermal expansion of the materials. To solve this problem UWA is investigating other alternatives, proposing the use of a niobium flexure [15]. This design requires cutting a small groove into the sapphire test mass. Measurements of Q-factor on sapphire test masses performed at UWA [16] showed that even with roughly cut grooves, the Q-factor is not dramatically affected, reaching values of $2.3 \times 10^8$.

## 5. Radiation pressure and optical spring effect

At the quantum level, the noise correlations between radiation pressure and intensity fluctuations can be used to suppress the total noise below the standard quantum limit [17]. At the classical level, the cross-coupling between intensity and radiation pressure can lead to various effects which include amplification or attenuation of perturbations, instabilities, bi-stability and mechanical frequency tuning effects. Their effects depend on the parameters of the opto-mechanical system.

During the third test at the HOPTF, the built-up power inside the cavity will be $\sim$200 kW. The radiation pressure force created by the transfer of momentum from photons will be of the order of 1.3 mN [18]. This is enough to cause the suspension pendulum to be deflected by 20 $\mu$m, about 40 times the cavity free spectral range [19]. This mirror displacement will modulate the light intensity inside the cavity changing the radiation pressure force. This change will act on the mirror resulting in a spring effect, with a spring constant depending on the frequency offset between the laser and the cavity resonance.

The optical spring effect was recently observed in a bench-top experiment at the ANU using a detuned Fabry–Perot resonator in which one mirror was mounted on a niobium flexure so that it could respond to radiation pressure [20]. The observed shift in the mechanical resonance due to the presence of the optical spring agreed with a simple model.

At UWA, two separate bench-top experiments are being conducted in order to measure and better understand the effects of high power lasers inside optical cavities [21]. These experiments are designed to study the effects of radiation pressure in suspended optics, optical spring effects and parametric instabilities in a high finesse optical cavity in a mechanical niobium resonator [22].

## 6. Thermal lensing

Any optical component in the presence of a laser beam will suffer some thermal lensing as a direct consequence of the power absorbed inside the substrate and coating. The temperature gradient that appears in the test mass substrates depends on the absorption level, the laser power density and is inversely proportional to the substrate thermal conductivity. These thermal effects will seriously degrade the performance of the advanced GW interferometers where very high power builds up inside the main cavities [23].

Inside the optics, the temperature gradient induces a refractive index gradient making the optics behave like a lens. Moreover, the substrate temperature gradient inside the material due to absorption will produce a non-uniform expansion. As a consequence of this expansion, the optical path length of the transmissive optics is increased, and the radius of curvature (ROC) in reflective optics is also increased.

In order to correct the very strong effect that will be induced in the test mass, continuing work previously done by LIGO [24] and GEO600 [25] groups, a fused silica lens mounted in a ring with controlled heating is proposed [26]. The temperature of the heating ring is adjusted to make the spatial variation in optical path length of the compensating plate exactly opposite to that of the input test mass (ITM).

## 7. The Hartmann wavefront sensor

Using a Hartmann plate, an opaque plate sustaining an array of holes, an array of light rays is generated. The rays propagate through the ITM and their positions are recorded using a CCD camera, thereby defining the reference positions. Absorption in the ITM creates a refractive index gradient within the ITM, which refracts the Hartmann rays. The transverse aberration of the rays is then used to calculate the wavefront distortion introduced by the ITM [27].

In order not to interfere with the optical mode of the cavity we use an off-axis Hartmann sensor, in which the Hartmann rays pass through the ITM at an angle to the longitudinal axis of the optical cavity. A schematic of the input test bench for the Gingin test 1 can be seen in

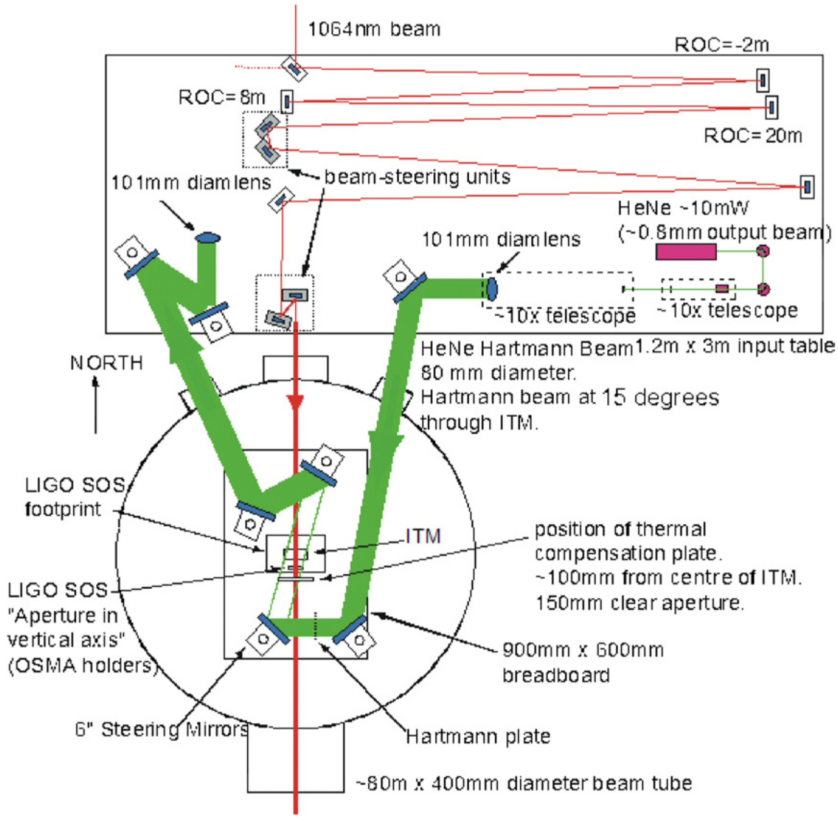


**Figure 3.** Schematic diagram that shows the distribution of the input test bench including the ITM and the Hartmann sensor inside the vacuum tank.

figure 3, where the location of the Hartmann plate is shown. A wavefront sensor will also be used to examine the eigenmodes of the optical cavities to reveal changes in mirror curvatures. These sensors are being tested in bench-top experiments at Adelaide University.

## 8. ACIGA high optical power tests

At the HOPTF, an 80 m half-symmetric Fabry–Perot cavity will be used to demonstrate and measure the effects of high laser power in advanced GW interferometry. In order to induce strong thermal effects in the first test, the ITM substrate will be inside the cavity as in figure 4(*a*).

These tests involve the following sub-systems. A pre-stabilized laser (PSL) locked to a 10 W laser that for future tests will be upgraded to 50 W. The input test bench includes the mode matching telescope and a He–Ne laser that will be used to measure the deformation and thermal lens of the ITM. The ITM made from *a*-axis sapphire is flat and has an anti-reflective coating (AR) with $R < 100$ ppm on the front surface and a $T = 1800$ ppm out-coupling coating on the back surface. The out-coupling coating is designed to maximize the power build up in the cavity, allowing for the substrate absorption and losses due to the AR coating on the ITM and compensation plate. The end test mass (ETM) made from *m*-axis sapphire has a 720 m ROC with a high reflectivity (HR) coating.

(*a*) Gingin Test 1:

(*b*) Gingin Test 2:

(*c*) Gingin Test 3:

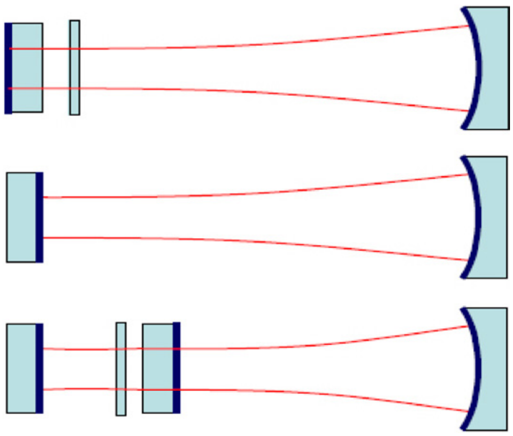

**Figure 4.** Gingin tests are designed with different purposes. Test 1 is to quantify and correct thermal lensing effects using two sapphire test masses and a fused silica compensation plate. Test 2 will use the same test masses to study thermal effects in the HR coating. Test 3 includes a fused silica power recycling mirror to increase the power in the cavity for further study of thermal effects and radiation pressure.

Around 7 W of laser power will be delivered to the cavity generating 5 kW inside. The ITM substrate will absorb 2 W of this power changing its ROC from flat to 350 m. This will change the size and position of the cavity waist. The waist radius will change from 8.75 mm to 6.62 mm and will move from the ITM HR coating 56 m to the centre of the cavity, reducing the power inside the cavity by about 20%. To restore the power, a fused silica lens mounted in a compensation plate has been designed. The compensation plate presented in section 6 will be used to counteract the thermal effect of the ITM substrate by creating a temperature gradient opposite to the one in the ITM. In parallel at the input test bench a mirror with a variable ROC will be used as part of the mode matching telescope for adaptive mode matching [28]. The aim is to dynamically correct the laser beam profile before entering the cavity. The final combined optical effect between the ITM and the compensation plate will be a virtually flat test mass. The cavity waist and mode matching will be set back to the cold cavity values, thereby restoring its power.

At the south arm of the HOPTF BK7 optics have been mounted in LIGO suspensions as ITM and ETM under vacuum. These are mounted on top of optical tables (figure 5) in order to characterize the optical system and lock the cavity using a 500 mW Nd:YAG laser, which later on will be replaced by a 10 W laser. The addition of a complete AIGO suspension system will be installed as soon as its digital control system is demonstrated. Figure 6 shows the locked cavity with both test masses inside their respective tanks.

The vacuum enclosure where this experiment is installed is formed by three 3.3 m height and 1.6 m diameter tanks connected by a ~80 m pipe. An intermediate tank already installed inside the main lab will be used during the third test, which includes a power recycling cavity (PRC). In this tank, we will install the ITM adding a fused silica power recycling mirror in the first tank. The whole vacuum enclosure has been pumped down to $2 \times 10^{-7}$ mbar with $8 \times 10^{-10}$ mbar total partial hydrocarbon pressure.

Gingin test 2 main objective is to test the effects of high laser power in the HR coating. Using the same test masses and leaving the ITM substrate outside the cavity (figure 4(*b*)) the power inside the cavity will be mainly absorbed by the HR coating. The laser power will be increased from 10 W to 50 W.

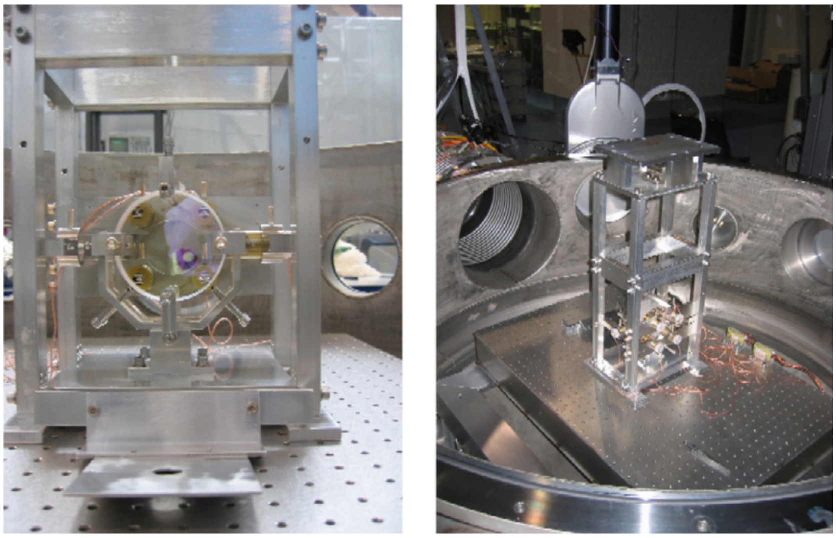

**Figure 5.** BK7 input test mass mounted on LIGO I suspension inside the tank just before closing it. The picture on the left was taken from the high reflection coating side, where it is possible to see the magnetic actuators behind the mirror.

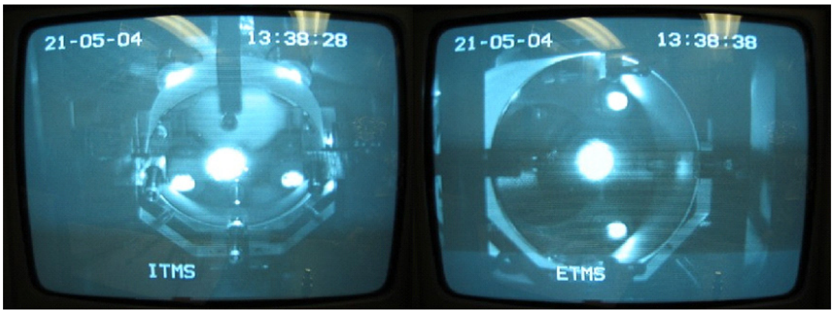


**Figure 6.** The pictures show the images from the CCD cameras mounted outside the vacuum tanks. The cameras are used to monitor the test masses during locking and operation. We can see the cavity locked and the fundamental mode reflected in both test masses.

With the addition of a fused silica mirror before the ITM to create a PRC as shown in figure 4(*c*), Gingin test 3 will work at even higher levels of power. The compensation plate will be used to reduce the thermal effects in the PRC. This configuration will allow us to study the effects of high power dynamics, and will also allow us to investigate radiation pressure and optical spring effects.

## 9. Summary

The tests presented here were designed to demonstrate and measure the effects of high power lasers in advanced GW detection. Different approaches and techniques have been developed in collaboration with the international community and the group members of ACIGA. As part of this collaboration ACIGA's research included different fields such as vibration isolation, thermal lensing, high power lasers, radiation pressure and optical spring. These results will help ACIGA to develop AIGO into the first advanced gravitational wave interferometer of the southern hemisphere, a key component of the international network of GW interferometers.

**Acknowledgments**

This work is supported by the Australian Research Council, the Department of Education, Science and Training (DEST) and by LIGO laboratories. The authors wish to thank the LIGO ACIGA Advisory Committee: Jordan Camp, Bill Kells, David J Ottaway, David Reitze, Benno Willke and Mike Zucker. Also acknowledged is David Shoemaker for his support of this committee. Mark Barton was supported by the US National Science Foundation under grant number PHY0245117. The authors also wish to thank the Gravity Waves technical staff at UWA: Ken Field, Peter Hay, Vinnie Nguyen, Xiaomei Niu, Steve Pople, Tim Slade, Daniel Stone and James Wakeling.

**References**

[1] Frede M, Wilhelm R, Gau R, Brendel M, Zawischa I, Fallnich C, Seifert F and Willke B 2004 High-power single-frequency Nd:YAG laser for gravitational wave detection *Class. Quantum Grav.* **21** S895–901
[2] Takeno K, Moriwaki S and Mio N 2004 Development of a high-power and stable laser for large-scale cryogenic gravitational wave telescope *Class. Quantum Grav.* **21** S881–6
[3] Mudge D, Veitch P J, Munch J, Ottaway D and Hamilton M W 1997 High-power diode-laser-pumped CW solid-state lasers using stable–unstable resonators *IEEE J. Sel. Top. Quantum Electron.* **3** 19–25
[4] Veitch P J, Mudge D, Hosken D and Munch J 2004 Lasers for gravitational wave interferometry *Gen. Rel. Grav. Preprint, Melbourne, 2004*
[5] Mudge D, Ostermeyer M, Ottaway D J, Veitch P J, Munch J and Hamilton M W 2002 High-power Nd:YAG lasers using stable−unstable resonators *Class. Quantum Grav.* **19** 1783–92
[6] Losurdo G *et al* 1999 An inverted pendulum preisolator stage for the VIRGO suspension system *Rev. Sci. Instrum.* **70** 2507–15
[7] Winterflood J 2001 High performance vibration isolation for gravitational wave detection *PhD Thesis* chapter 6, The University of Western Australia, School of Physics, Perth
[8] Takamori A *et al* 2002 Mirror suspension system for the TAMA SAS *Class. Quantum Grav.* **19** 1615–21
[9] Go$\beta$ler *et al* 2002 The modecleaner system and suspension aspects of GEO 600 *Class. Quantum Grav.* **19** 1835–42
[10] Winterflood J 2001 High performance vibration isolation for gravitational wave detection *PhD Thesis* chapter 7, The University of Western Australia, School of Physics, Perth
[11] Garoi F, Winterflood J, Ju L, Jacob J S and Blair D G 2003 Passive vibration isolation using a Roberts linkage *Rev. Sci. Instrum.* **74** 3487–91
[12] Winterflood J, Barber T and Blair D G 2002 Using Euler bucklings springs for vibration isolation *Class. Quantum Grav.* **19** 1639–45
[13] Kuroda K *et al* 1999 Large-scale cryogenic gravitational wave telescope *Int. J. Mod. Phys.* D **8** 557–79
[14] Yan Z, Ju L, Eon F, Gras S, Zhao C, Jacob J S and Blair D G 2004 Large scale inhomogeneity in sapphire test masses revealed by Rayleigh scattering imaging *Class. Quantum Grav.* **21** S1139–44
[15] Ju L, Blair D G, Bilenko I and Paget D 2002 Low loss niobium flexure suspension systems *Class. Quantum Grav.* **19** 1703–8
[16] Gras S, Ju L and Blair D G 2004 Influence of grooves and defects on the sapphire test mass Q-factor *Class. Quantum Grav.* **21** S1121–6
[17] Buonnano A and Chen Y 2001 Quantum noise in second generation, signal-recycled laser interferometric gravitational-wave detectors *Phys. Rev.* D **64** 042006
[18] Jacob J S *et al* 2003 Australia's role in gravitational wave detection *Publ. Astron. Soc. Aust.* **20** 223–41
[19] Ju L *et al* 2004 ACIGA's high optical power test facility *Class. Quantum Grav.* **21** S887–93
[20] Sheard B S, Gray M B, Mow-Lowry C, McClelland D E and Whitcomb S E 2004 Observation and characterization of an optical spring *Phys. Rev.* A **69** 051801(R)
[21] Garoi F, Ju L, Zhao C and Blair D G 2004 Radiation pressure actuation of test masses *Class. Quantum Grav.* **21** S875–80

[22] Schediwy S W, Zhao C, Ju L and Blair D G 2004 An experiment to investigate optical spring parametric instability *Class. Quantum Grav.* **21** S1253–8

[23] McClelland D E, Camp J B, Mason J, Kells W and Whitcomb S E 1999 Arm cavity resonant sideband control for laser interferometric gravitational wave detectors *Opt. Lett.* **24** 1014–6

[24] Lawrence C R 2003 Active wavefront correction in laser interferometric gravitational wave detectors *PhD Thesis* Massachusetts Institute of Technology

[25] Lück H, Freise A, Go$\beta$ler , Hild S, Kawabe K and Danzmann K 2004 Thermal correction of the radii of curvature of mirrors for GEO600 *Class. Quantum Grav.* **21** S985–9

[26] Degallaix J, Zhao C, Ju L and Blair D G 2004 Thermal lensing compensation for AIGO high power test facility *Class. Quantum Grav.* **21** S903–8

[27] Brooks A, Kelly T L, Veitch P J and Munch J 2004 Development of wavefront distortion sensors for Gingin high power test facility *Gen. Rel. Grav. Preprint, Melbourne, 2004*

[28] Degallaix J, Zhao C and Blair D G 2004 Thermal lensing compensation principle for the High Optical Power Test Facility Test 1 *Gen. Rel. Grav. Preprint, Melbourne, 2004*